

MEASURING COSMIC DISTANCES WITH GALAXY CLUSTERS

S. W. Allen^{1,2,3}, A. B. Mantz^{4,5}, R. G. Morris^{1,3}, D. E. Applegate⁶,
P. L. Kelly⁷, A. von der Linden^{1,2,8}, D. A. Rapetti⁸, R. W. Schmidt⁹

¹Kavli Institute for Particle Astrophysics and Cosmology

²Department of Physics, Stanford University, 382 Via Pueblo Mall, Stanford, CA 94305, USA

³SLAC National Accelerator Laboratory, 2575 Sand Hill Road, Menlo Park, CA 94025, USA

⁴Kavli Institute for Cosmological Physics

⁵Department of Astronomy and Astrophysics, University of Chicago, 5640 South Ellis Avenue, Chicago, IL 60637, USA

⁶Argelander-Institute for Astronomy, Auf dem Hugel 71, D-53121 Bonn, Germany

⁷Department of Astronomy, University of California, Berkeley, CA 94720-3411, USA

⁸Dark Cosmology Centre, Niels Bohr Institute, University of Copenhagen, Juliane Maries Vej 30, DK-2100 Copenhagen, Denmark

⁹Astronomisches Rechen-Institut, Zentrum fur Astronomie der Universitat Heidelberg, Monchhofstrasse 12-14, 69120 Heidelberg, Germany

Abstract:

In addition to cosmological tests based on the mass function and clustering of galaxy clusters, which probe the growth of cosmic structure, nature offers two independent ways of using clusters to measure cosmic distances. The first uses measurements of the X-ray emitting gas mass fraction, which is an approximately standard quantity, independent of mass and redshift, for the most massive clusters. The second uses combined millimeter (mm) and X-ray measurements of cluster pressure profiles. We review these methods, their current status and the prospects for improvements over the next decade. For the first technique, which currently provides comparable dark energy constraints to SNIa studies, improvements of a factor of 6 or more should be readily achievable, together with tight constraints on Ω_m that are largely independent of the cosmological model assumed. Realizing this potential will require a coordinated, multiwavelength approach, utilizing new cluster surveys, X-ray, optical and mm facilities, and a continued emphasis on improved hydrodynamical simulations.

1 Introduction

Cosmological tests based on observations of galaxy clusters have seen tremendous improvement in recent years (Allen, Evrard & Mantz 2011; Fig. 1a), setting competitive constraints on cosmological parameters including the amplitude of the matter power spectrum (σ_8), the mean matter and dark energy densities (Ω_m and Ω_{DE}), the dark energy equation of state, w (Allen et al., 2008; Vikhlinin et al., 2009; Mantz et al., 2010b; Rozo et al., 2010; Benson et al., 2013), departures from General Relativity on cosmological scales (Schmidt, Vikhlinin & Hu, 2009; Rapetti et al., 2010, 2013), and the species-summed neutrino mass (Mantz, Allen & Rapetti, 2010; Reid et al., 2010).

In addition to tests based on measurements of the mass function and clustering of galaxy clusters (Vikhlinin et al., 2009; Mantz et al., 2010b; Rozo et al., 2010; Weinberg et al., 2012; Benson et al., 2013), which are discussed elsewhere in these white papers, are two complementary ways of using galaxy clusters to measure cosmic distances. Both of these techniques use X-ray observations. The first and most powerful employs measurements of the X-ray gas mass fraction in clusters, which is a standard quantity for massive clusters, with minimal scatter from system to system (Allen et al.

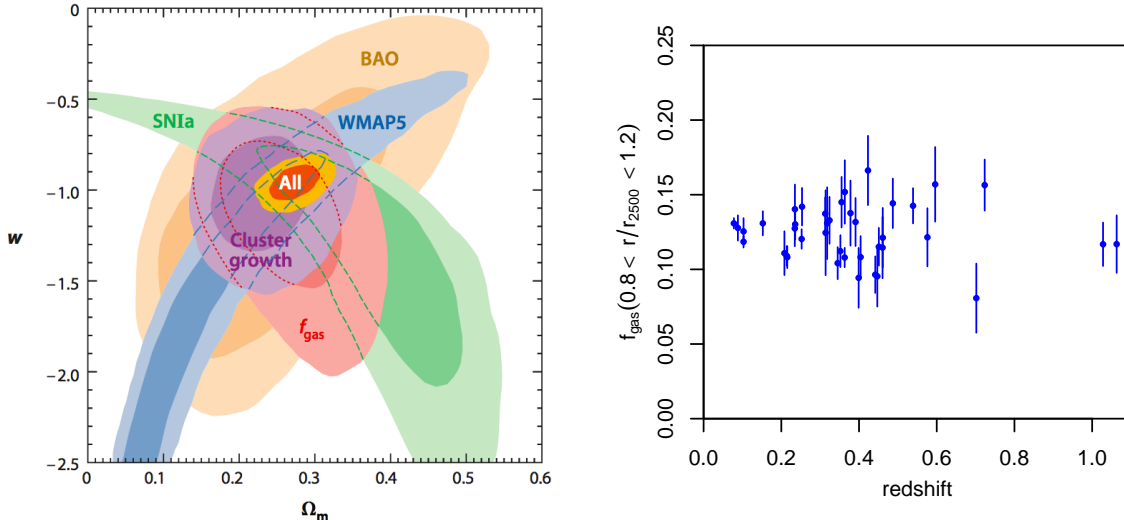


Figure 1: (a; left panel) Cosmological constraints from galaxy clusters and other probes. Joint 68.3% and 95.4% confidence constraints on the dark energy equation of state, w , and mean matter density, Ω_m , from the observed abundance and growth galaxy clusters (Mantz et al., 2010b) and cluster f_{gas} measurements (Allen et al., 2008), compared with those from the Wilkinson Microwave Anisotropy Probe (WMAP; Dunkley et al. 2009), type Ia supernovae (SNIa; Kowalski et al. 2008) and baryon acoustic oscillations (BAO; Percival et al. 2010) for spatially flat, constant w models. Gold contours show the results from the combination of all data sets (Allen, Evrard & Mantz, 2011). (b; right panel) f_{gas} measurements in the $0.8-1.2 r_{2500}$ shell for the 40 hottest ($kT \gtrsim 5\text{keV}$), most dynamically relaxed clusters known (Mantz et al., 2013). For illustration, cosmology-dependent quantities are plotted (for an $\Omega_m = 0.3$, $\Omega_\Lambda = 0.7$, $h = 0.7$ Λ CDM reference cosmology), although in practice model predictions are compared with cosmology-independent measurements.

2004, 2008; Battaglia et al. 2012; Mantz et al. 2013). The second technique employs combined X-ray and mm-wavelength measurements of the thermal pressure profiles in clusters, utilizing the Sunyaev-Zel'dovich effect (Carlstrom, Holder & Reese, 2002).

This white paper briefly describes these two methods to measure cluster distances, their current status, and the prospects for improvement over the next decade.

2 Distance measurements from the cluster X-ray gas mass fraction

2.1 Overview and current status

The matter content of the most massive galaxy clusters is expected to provide an almost fair sample of the matter content of the Universe. The ratio of baryonic-to-total mass in these clusters should, therefore, closely match the ratio of the cosmological parameters Ω_b/Ω_m . The baryonic mass content of clusters is dominated by the X-ray emitting gas, the mass of which exceeds the mass in stars by an order of magnitude (e.g. Giodini et al. 2009) with other sources of baryonic matter being negligible. The combination of robust measurements of the baryonic mass fraction in clusters from X-ray observations, with a determination of Ω_b from cosmic microwave background (CMB) data or big-bang nucleosynthesis calculations and a constraint on the Hubble constant, can therefore be used to measure Ω_m (e.g. White et al. 1993). This method currently provides one of our best constraints on Ω_m , and is simple and robust in terms of its underlying assumptions.

Measurements of the apparent evolution of the cluster X-ray gas mass fraction, hereafter f_{gas} , can also be used to probe the acceleration of the Universe (Allen et al. 2004, 2008; LaRoque et al. 2006; Ettori et al. 2009; Mantz et al. 2013). This constraint originates from the dependence of the

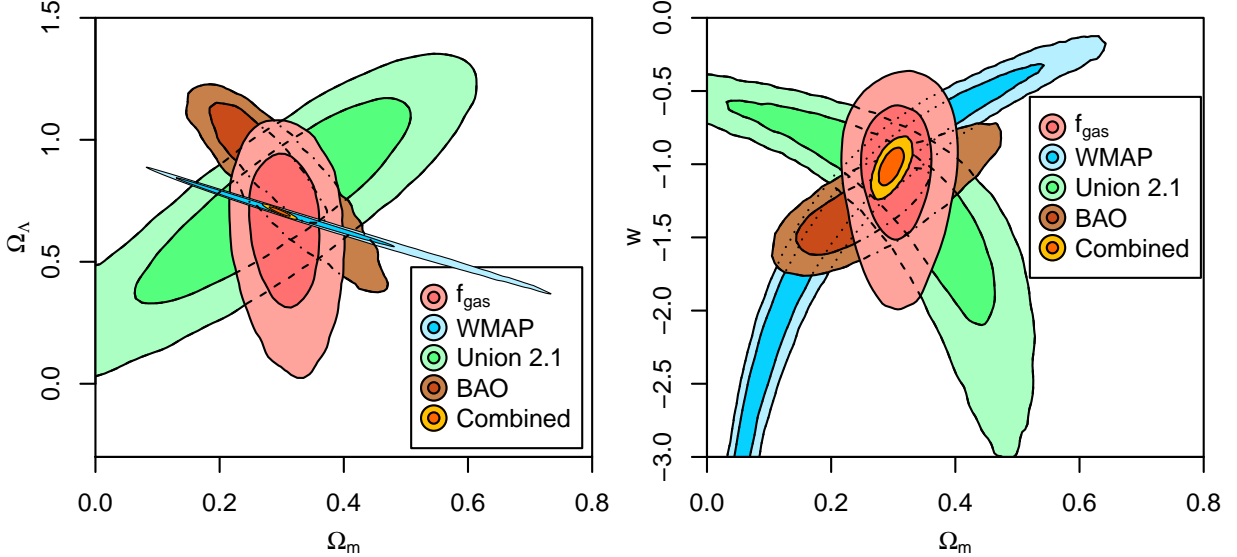


Figure 2: Joint 68.3% and 95.4% confidence constraints for non-flat Λ CDM (left) and flat w CDM (right) models. Red shading indicates confidence regions from current f_{gas} data (Mantz et al. 2013; employing standard priors on $\Omega_b h^2$ and h as described in Section 5.3.1). Independent constraints from CMB measurements (blue; Hinshaw et al. 2012), SN Ia (green; Suzuki et al. 2012), and BAO (brown; Anderson et al. 2013) are also shown.

f_{gas} measurements, which derive from the observed X-ray gas temperature and density profiles, on the assumed distances to the clusters, $f_{\text{gas}} \propto d^{1.5}$. The expectation from hydrodynamical simulations is that for the hottest, most massive systems, and for measurement radii (corresponding to a given overdensity¹) beyond the innermost core ($r \gtrsim r_{2500}$), f_{gas} should be approximately constant with redshift (Battaglia et al. 2012; Planelles et al. 2013; and references therein). Together, the expected behavior of $f_{\text{gas}}(z)$ and distance dependence of the measurements allow the distances to clusters to be inferred.

The first detection of cosmic acceleration using the f_{gas} technique was made by Allen et al. (2004). This work was extended by Allen et al. (2008, see also LaRoque et al. 2006; Ettori et al. 2009) and most recently by Mantz et al. (2013) using Chandra X-ray observations of 40 hot ($kT \gtrsim 5\text{keV}$), massive, dynamically relaxed clusters spanning the redshift range $0 < z < 1.1$. The total Chandra exposure used by Mantz et al. (2013), after all screening procedures are applied, is ~ 3.1 Ms. The f_{gas} measurements from the Mantz et al. (2013) study are shown in Fig. 1b. Fig. 2 shows the constraints from these data for a non-flat Λ CDM model (left panel; $\Omega_m = 0.31 \pm 0.04$, $\Omega_\Lambda = 0.69_{-0.24}^{+0.17}$) and a flat, constant- w model (right panel; $\Omega_m = 0.31 \pm 0.04$, $w = -0.99_{-0.32}^{+0.26}$). In both cases, the results are marginalized over conservative systematic uncertainties (Section 5.3). The f_{gas} constraints provide comparable constraints on dark energy to current SN Ia measurements (Suzuki et al., 2012), and an impressively tight constraint on Ω_m .

2.2 Modeling the f_{gas} data

We define f_{gas} as the ratio of the X-ray emitting gas mass to the total mass of a cluster, measured at a given overdensity. This quantity can be determined directly from X-ray observations under the assumptions of spherical symmetry and hydrostatic equilibrium. To ensure that these assumptions

¹The overdensity, or ratio of the mean matter density enclosed by a sphere to the critical density of the Universe, provides a convenient way to define characteristic radii of clusters. We typically write $M(< r_\Delta) = (4\pi/3) \Delta \rho_{\text{cr}}(z) r_\Delta^3$, with, for example, r_{2500} being roughly 1/4 the radius of the virialized region.

are as accurate as possible, it is essential to limit the f_{gas} analysis to the most dynamically relaxed clusters (Allen et al. 2004, 2008; Mantz et al. 2013). A further restriction to the hottest, most X-ray luminous systems simplifies the cosmology analysis and minimizes the required exposure times (see also Section 4).

Mantz et al. (2013) use Chandra f_{gas} measurements for a sample of 40 of the hottest ($kT_{2500} > 5$ keV), most dynamically relaxed clusters known. The selection on dynamical relaxation state is based on quantitative morphological criteria computed from X-ray images (Section 4). The f_{gas} measurements are made within a spherical shell spanning the radial range $0.8\text{--}1.2 r_{2500}$ (angular range $0.8\text{--}1.2 \theta_{2500}^{\text{ref}}$), determined for a chosen reference cosmology.

Hydrodynamical simulations, tuned to match the observed thermodynamic properties and scaling relations of galaxy clusters (e.g. Battaglia et al. 2012; Planelles et al. 2013) suggest that for the hottest, most massive clusters, and for measurement radii beyond the innermost core, the true gas mass fraction at a given overdensity should be approximately constant in mass and redshift,

$$f_{\text{gas}}(z; \theta_{2500}) = \Upsilon_{2500} \left(\frac{\Omega_{\text{b}}}{\Omega_{\text{m}}} \right), \quad (1)$$

where Υ_{2500} , also known as the gas depletion parameter, is the average ratio of the cluster gas mass fraction to the cosmic mean baryon fraction at the appropriate radii.

In comparing with data, an angular correction factor, A , is required to account for the fact that $\theta_{2500}^{\text{ref}}$ for the reference cosmology and θ_{2500} for a given trial cosmology are not identical. Observations show that over the radial range of interest, the $f_{\text{gas}}(r)$ profiles of hot, relaxed clusters can be described by a power-law model, independent of the reference cosmology (Allen et al., 2008). The f_{gas} measurements in the reference cosmology can then be related to a predicted curve for a particular trial cosmology, $f_{\text{gas}}^{\text{ref}}(z)$, through the relation

$$f_{\text{gas}}^{\text{ref}}(z; \theta_{2500}^{\text{ref}}) = A \Upsilon_{2500} \left(\frac{\Omega_{\text{b}}}{\Omega_{\text{m}}} \right) \left(\frac{d_{\text{A}}^{\text{ref}}}{d_{\text{A}}} \right)^{3/2}, \quad (2)$$

where

$$A = \left(\frac{\theta_{2500}^{\text{ref}}}{\theta_{2500}} \right)^{\eta} \sim \left(\frac{[H(z) d_{\text{A}}(z)]}{[H(z) d_{\text{A}}(z)]^{\text{ref}}} \right)^{\eta}. \quad (3)$$

For the $0.8\text{--}1.2 \theta_{2500}$ shell, $\eta = 0.442 \pm 0.035$ (Mantz et al., 2013). The explicit appearance of Ω_{m} in equation (2) means that low-redshift clusters (for which the dependence of d_{A} on the details of dark energy is negligible), in combination with external priors on $\Omega_{\text{b}} h^2$ and h , provide a tight and essentially model-independent constrain on Ω_{m} .

Following Allen et al. (2008), we extend equation (2) to also include allowances for systematic uncertainties,

$$f_{\text{gas}}^{\text{ref}}(z; \theta_{2500}^{\text{ref}}) = K A \Upsilon_{2500} \left(\frac{\Omega_{\text{b}}}{\Omega_{\text{m}}} \right) \left(\frac{d_{\text{A}}^{\text{ref}}}{d_{\text{A}}} \right)^{3/2}. \quad (4)$$

Here K is a systematic uncertainty on the overall normalization of the curve, encompassing terms relating to (among other factors) instrumental calibration and the expected mean level of non-thermal pressure support in the measurement shell (Mantz et al., 2013). Fortunately, the value of K can be constrained robustly through combination with independent weak lensing mass measurements for the target clusters, with current uncertainties at the ten per cent level ($K = 0.94 \pm 0.09$; Applegate et al. 2013). Note that only the mean level of these systematic effects is modeled by K ; cluster-to-cluster scatter is manifested as intrinsic scatter in the measurements.

The gas depletion parameter, Υ , reflects the thermodynamic history of the X-ray emitting cluster gas over the history of cluster formation. Systematic uncertainties are present in both the normalization and evolution of this parameter, although these uncertainties are minimized by our use of a measurement shell as opposed to traditional measurements within enclosed spheres (i.e. including cluster centers).² Defining a simple evolutionary model, $\Upsilon_{2500} = \Upsilon_0(1 + \alpha_\Upsilon z)$, recent hydrodynamic simulations spanning a range of plausible astrophysical models (Battaglia et al., 2012; Planelles et al., 2013) show that, for the hottest clusters and measurement shells $0.8\text{--}1.2 r_{2500}$, the full range of uncertainty is conservatively spanned by $\Upsilon_0 = 0.845 \pm 0.042$ and $\alpha_\Upsilon = 0.00 \pm 0.05$ (uniform priors).

We note that it is straightforward to additionally model the intrinsic scatter in f_{gas} measurements as well as a possible dependence of the mean $f_{\text{gas}}(z)$ on mass, constraining these terms simultaneously with the cosmological parameters. Mantz et al. (2013) place constraints on the intrinsic scatter (see Section 5.1), and confirm the expectation that the mean f_{gas} in the $0.8\text{--}1.2 r_{2500}$ shell is independent of mass.

3 Distance measurements from SZ and X-ray pressure profiles

3.1 Overview and current status

Cosmic microwave background (CMB) photons passing through a galaxy cluster have a non-negligible chance to inverse Compton scatter off the hot, X-ray emitting gas. This scattering boosts the photon energy and gives rise to a small but significant frequency-dependent shift in the CMB spectrum observed through the cluster, known as the thermal Sunyaev-Zel'dovich (hereafter SZ) effect (Sunyaev & Zeldovich, 1972).

Silk & White (1978) noted that X-ray and SZ measurements could in principle be combined to determine distances to galaxy clusters. The spectral shift to the CMB due to the SZ effect can be written in terms of the Compton y -parameter, which is a measure of the integrated electron pressure along the line of sight, $y \propto \int n_e T dl$. Given an observed SZ signal at mm or radio wavelengths, and a predicted SZ signal from X-ray measurements of the gas density and temperature profiles then, given the distance dependence of the X-ray measurements, we can solve for d_A .

This test, sometimes referred to as the XSZ (or SZX) test, is intrinsically less powerful than the f_{gas} test due to the cosmological signal being proportional to $d_A^{0.5}$, rather than $d_A^{1.5}$.³ As a result, the XSZ test has to date only been used to constrain the Hubble parameter. Bonamente et al. (2006) used this method to measure the distances to 38 X-ray luminous clusters spanning the redshift range $0.14 < z < 0.89$. Assuming spatial flatness and fixing $\Omega_m = 0.3$, they determined a Hubble parameter, $h = 0.77^{+0.11}_{-0.09}$, consistent with the results from the Hubble Key Project ($h = 0.72 \pm 0.08$; Freedman et al. 2001).

3.2 Modeling the XSZ data

For the true, underlying cosmology, the measurements of the Compton y -parameter from the X-ray and mm-wavelength data should be equal. For a given cosmology, the y -parameter determined from the X-ray data depends on the square root of the angular diameter distance to the cluster, whereas the observed SZ flux at mm (or radio) wavelengths is independent of the cosmology assumed. Combining these y -parameter results, we can measure the distances to the clusters as a function of

²Systematic uncertainties in the prediction of Υ , which are primarily related to uncertainties in the baryonic physics, mainly affect the innermost regions of clusters at $r < 0.5r_{2500}$.

³As discussed in this document, the f_{gas} test also provides a second, independent constraint on Ω_m from the fair sample argument.

redshift:

$$y_X^{\text{ref}} = y_{\text{SZ}} k(z) \left(\frac{d_A^{\text{ref}}}{d_A} \right)^{1/2}. \quad (5)$$

Here y_X^{ref} is the X-ray measurement of the y -parameter for a reference cosmology and y_{SZ} is the cosmology-independent mm (or radio) observation. Following a similar approach to the f_{gas} case, we again incorporate systematic allowances into equation (5), via the term $k(z) = k_0(1 + \alpha_k z)$, which in this case accounts for the combined uncertainties due to instrument calibration, geometric effects, gas clumping and their evolution. Again, only the mean level of these systematic effects is modeled by $k(z)$; cluster-to-cluster scatter will be manifested as intrinsic scatter in the measurements.

4 The optimal cluster targets

A simplifying aspect of the f_{gas} and XSZ methods is that the optimal targets for both experiments are identical. In each case, the ideal targets are the most massive – and therefore hottest and most X-ray luminous – dynamically relaxed clusters.

X-ray images with modern X-ray telescopes (point spread functions of ~ 10 arcsec or better) allow for the straightforward assessment of the dynamical states of clusters based on measurements of the peakiness and symmetry of the X-ray emission, and the level of isophote centroid variation. This selection can be easily automated (e.g. Mantz et al. 2013).⁴ Existing Chandra and XMM-Newton data for clusters at $0 < z < 1.1$ indicate that approximately 1/8 clusters with $kT > 5$ keV can be classified as highly relaxed (Mantz et al., 2013).

From the f_{gas} perspective, the restriction to the most dynamically relaxed clusters, for which the assumptions of hydrostatic equilibrium and spherical symmetry should be most valid, minimizes the systematic scatter in the f_{gas} measurements, which in turn impacts on the cosmological constraining power. The restriction to the most massive clusters additionally simplifies the prediction of the gas depletion factor, $\Upsilon(z)$: for clusters with $kT > 5$ keV and for the measurement radii of interest ($0.8\text{--}1.2 r_{2500}$) the depletion factor is predicted to be essentially independent of mass and redshift and to exhibit minimal intrinsic scatter from cluster to cluster (Battaglia et al., 2012; Planelles et al., 2013; Mantz et al., 2013). Since the most massive clusters are also the most luminous at a given redshift, these targets will require the shortest exposure to reach a given X-ray measurement precision. Likewise, from the XSZ perspective, the restriction to the hottest, most dynamically relaxed clusters maximizes the X-ray and mm-wavelength signals and minimizes the systematic uncertainties associated with geometry and substructure/clumping.

5 Prospects for improvement

5.1 An observing program for cluster distance measurements

Future f_{gas} and XSZ experiments will build upon new cluster surveys. Together, these surveys will map the whole sky, finding in excess of 100,000 clusters, including thousands of hot, massive systems out to high redshifts. Fig. 3a shows the predicted distribution of clusters with temperature $kT > 5$ keV as a function of redshift.

After completing its 4-year X-ray survey, the eROSITA mission (Merloni et al., 2012) will spend at least two more years carrying out targeted, follow-up observations to measure low-scatter X-ray mass proxies: X-ray temperatures (kT), gas masses (M_{gas}), and Y_X values (the product of

⁴In principle, future X-ray missions with larger collecting area and higher spectral resolution could also utilize measurements of gas motions within clusters and/or thermodynamic maps to assess their dynamical states.

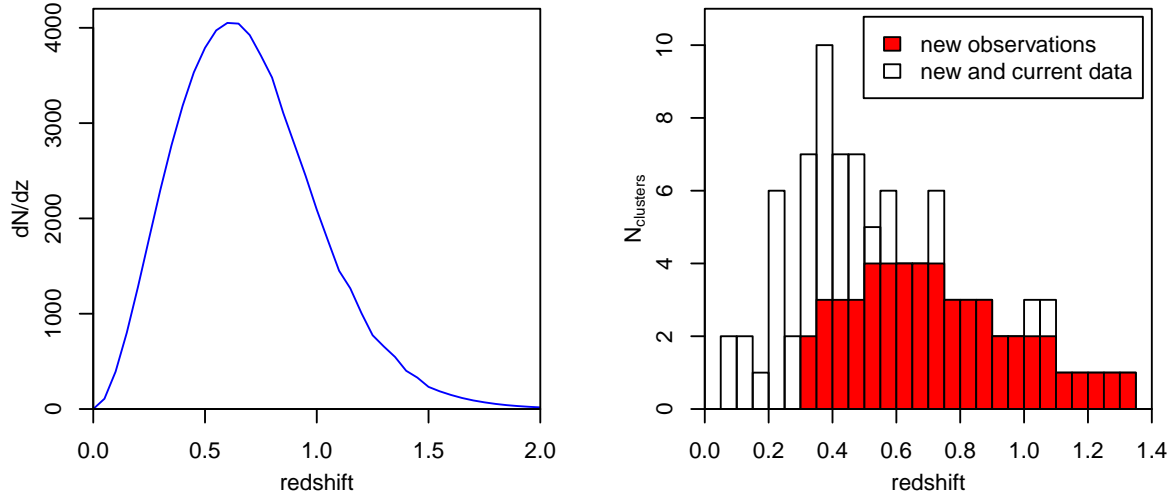


Figure 3: (*a; left panel*) Differential number of clusters with temperatures $kT > 5$ keV predicted to be detected by the eROSITA survey. We assume a concordance Λ CDM model with the halo mass function of Tinker et al. (2008), cluster luminosity and temperature scaling relations measured by Mantz et al. (2010a), and a survey flux limit of 3.3×10^{-14} erg s $^{-1}$ cm $^{-2}$ in the 0.5–2.0 keV band. (*b; right panel*) The red histogram shows a plausible redshift distribution for new cluster observations achievable with 10 Ms of Chandra time over the next decade. These represent a fair sample of the distribution shown in the left panel at $z \geq 0.3$. The union of these future observations with the current data set of Mantz et al. (2013) is shown in the white histogram. This has been used in projecting future cosmological constraints (Section 5.4).

gas mass and temperature; Allen, Evrard & Mantz 2011). The addition of such low-scatter mass proxy measurements for even a small fraction of the clusters in a survey can in principle boost the cosmological constraining power by a factor of a few with respect to self-calibration of the mass function and clustering data alone (Wu, Rozo & Wechsler, 2010). Of order a thousand follow-up measurements are likely to be made with eROSITA, gathering 1000 or more counts per target. In many cases these observations will also be sufficient to assess the dynamical states of the clusters.

The hottest, most X-ray luminous, dynamically relaxed clusters identified in this way will be the targets for further, deeper follow-up by flagship X-ray observatories and SZ telescopes, designed to enable the f_{gas} and XSZ experiments. For simplicity, we assume here that this deeper X-ray follow-up will be carried out exclusively with Chandra, utilizing an observing budget of 10 Ms over the next decade (approximately 5% of the available satellite observing time).

Mantz et al. (2013) determine an intrinsic scatter in f_{gas} measurements for the hottest, most relaxed clusters at $0 < z < 1.1$ in the $0.8\text{--}1.2 r_{2500}$ shell of $7.4\% \pm 2.3\%$. This implies an intrinsic scatter in the distance measurements to individual clusters of $\sim 5\%$. Since it is inefficient for f_{gas} measurements of individual clusters to exceed this precision significantly, we propose a target precision for future Chandra f_{gas} measurements (in the same shell) of $\sim 15\%$. The required exposure times for individual targets can be estimated straightforwardly from existing data.⁵

Fig. 3b shows the redshift histogram of a possible target list of hot ($kT > 5$ keV), relaxed clusters that could be observed in 10 Ms of Chandra time. The targets are drawn fairly from the full distribution shown in Fig. 3a, apart from the requirement that $z \geq 0.3$. The fiducial parameter values used to simulate these data are shown in Table 2. Exposure times are tuned to provide a precision in f_{gas} of $\sim 15\%$ in the $0.8\text{--}1.2 r_{2500}$ shell, with the maximum exposure per cluster

⁵Based on the existing Chandra data, the exposure time, t , needed to reach a given fractional uncertainty on f_{gas} , ε , in the $0.8\text{--}1.2 r_{2500}$ measurement shell for a cluster at redshift z is well approximated by $t = (5.65 \times 10^{-7} \text{ ks}) [d_L(z)/\text{Mpc}]^2 \varepsilon^{-2} E(z)^{-2.3}$, where $E(z) = H(z)/H_0$ and $d_L(z)$ is the luminosity distance.

limited to 300 ks ⁶. In total ~ 53 new clusters can be observed in this way. When combined with current data (Mantz et al., 2013), this gives a sample of ~ 93 measurements meeting the target precision over the redshift range $0 < z < 1.4$. Our simulations of projected cosmology constraints for the f_{gas} experiment (Section 5.4) are carried out for this combined data set.

For the XSZ test, which does not require information on the gas depletion factor, it is efficient to use a wider shell, encompassing most of the sphere enclosed within $1.2r_{2500}$ (excluding just a small central region of radius $r < 0.2r_{2500}$). The Chandra X-ray observations described above, which are intended to measure f_{gas} in the $0.8\text{--}1.2r_{2500}$ shell to $\sim 15\%$ precision, should also enable $y_{\text{X}}^{\text{ref}}$ to be measured to $\sim 7.5\%$. However, given the larger level of intrinsic scatter expected in the XSZ measurements ($\sim 20\%$, corresponding to 40% in distance), due primarily to the impact of triaxiality and projection effects on the measured y_{SZ} values (Bonamente et al., 2006; Hallman et al., 2007; Shaw, Holder & Bode, 2008), it is likely that the shallower eROSITA X-ray data set described above, which will contain many more clusters, will be at least as useful for this work. Envisaging some modest restriction in the XSZ target selection on the basis of dynamical state, we have simulated an XSZ data set appropriate for 500 eROSITA clusters, fairly sampling the dN/dz curve in Fig. 3a at redshifts $z > 0.1$, with X-ray measurements made to 20% precision (roughly the minimum precision necessary to measure a useful mass proxy). We assume that the accompanying, targeted mm observations, made with facilities such as CARMA⁷ or CCAT⁸, will have significantly greater precision. Our projected cosmology constraints for the XSZ experiment (Section 5.4) are for this data set.

5.2 Figure of merit

We quantify the improvements in cosmological constraining power with the proposed observing strategy for three cosmological models: non-flat Λ CDM, flat w CDM (i.e. a flat dark energy model with a constant equation of state, w) and a flat, evolving dark energy model with $w(a) = w_0 + w_a(1 - a)$, where a is the scale factor, similar to that employed by the Dark Energy Task Force (DETF; Albrecht et al. 2006). For each model, our figure of merit is defined as the inverse of the area enclosed by the 95.4% confidence contour for the associated pair of parameters $[(\Omega_{\text{m}}, \Omega_{\Lambda}), (\Omega_{\text{DE}}, w)$ or (w_0, w_a) , respectively], normalized by the constraints provided by current data (Mantz et al., 2013). We also examine the fractional uncertainty in the marginalized constraint on Ω_{m} , which is well constrained by the data.

As with the real data, our determination of projected constraints employs the Metropolis Markov Chain Monte Carlo (MCMC) algorithm implemented in the COSMOMC⁹ code (Lewis & Bridle, 2002) to determine posterior parameter distributions. This ensures maximal consistency in our calculation of figures of merit, and that we capture fully the various degeneracies between model parameters and priors (Wolz et al. 2012). Note that, as a result, our figure of merit differs slightly from that introduced by the DETF, in which a Gaussian approximation to the posterior is used to estimate the area enclosed by the confidence contours. We measure the area enclosed directly from Monte Carlo simulations of the posterior, including all details of its shape.¹⁰

⁶Exposure times of this length are also well suited to a broad range of astrophysical studies, for example studies of the incidence, properties and evolution of cool cores, which may have high priority in the community (e.g. Siemiginowska et al. 2010; Santos et al. 2012; McDonald et al. 2013). Alternatively, the same 10 Ms exposure time could be divided among, e.g., twice as many new clusters, leading to similar cosmological constraints.

⁷<http://www.mmarray.org/>

⁸<http://www.ccatobservatory.org/>

⁹<http://cosmologist.info/cosmomc/>

¹⁰A previous study of the potential of the f_{gas} and XSZ experiments, carried out in the context of the planned Constellation-X and XEUS satellites, was presented by Rapetti, Allen & Mantz (2008). Their analysis employed the

Table 1: Systematic allowances on parameters, expressed as fractions of their fiducial values (see Table 2).

Parameter	Current	Future		Form
		pessimistic	optimistic	
$\Omega_b h^2$	± 0.04	± 0.04	± 0.01	Gaussian
h	± 0.03	± 0.03	± 0.01	Gaussian
K	± 0.10	± 0.05	± 0.02	Gaussian
Υ_0	± 0.05	± 0.05	± 0.02	Uniform
α_Υ	± 0.05	± 0.05	± 0.02	Uniform
k_0	± 0.12	± 0.05	± 0.02	Gaussian
α_k		± 0.05	± 0.02	Uniform

Table 2: Fiducial parameter values used to simulate future cluster data.

$h = 0.7$	$\Upsilon_0 = 0.845$
$\Omega_b = 0.045$	$\alpha_\Upsilon = 0.0$
$\Omega_m = 0.3$	$K = 1.0$
$\Omega_\Lambda = 0.7$	$k_0 = 1.0$
$w_0 = -1.0$	$\alpha_k = 0.0$
$w_a = 0.0$	

5.3 Priors and systematic allowances

In order to keep the interpretation of projected results as simple as possible, we present results for two sets of priors and systematic allowances, corresponding to pessimistic and optimistic (standard) scenarios.

5.3.1 f_{gas} method

Cosmological analyses based on f_{gas} data alone require external priors on $\Omega_b h^2$ and h . The current analysis (Mantz et al., 2013) uses $\Omega_b h^2 = 0.0223 \pm 0.0009$ (Pettini & Cooke, 2012) and $h = 0.738 \pm 0.024$ (Riess et al., 2011). Our pessimistic assumption is that this will not improve. Optimistically, we assume that CMB and other data will improve these priors to the $\sim 1\%$ level over the next decade. Note that when combining f_{gas} and CMB data directly, external priors on $\Omega_b h^2$ and h are not required.

The calibration prior for the f_{gas} analysis, K , can be constrained robustly using weak lensing measurements for the target clusters. Current uncertainties in the value of this prior are at the 10% level ($K = 0.94 \pm 0.09$; Applegate et al. 2013), with no evidence for evolution, and are limited by the small number of hot, relaxed clusters with rigorous weak lensing mass measurements. The path toward improving this constraint appears straightforward, however, with programs to gather additional lensing data, and to improve the accuracy of the shear calibration and lens modeling, underway (von der Linden et al., 2012; Kelly et al., 2012; Applegate et al., 2012). Optimistically,

standard DETF figure of merit, calculated from MCMC chains, and Planck simulated data. However, it underestimated the progress in mitigating systematic uncertainties; in particular, the pessimistic scenarios considered by those authors can now be excluded.

calibration of K at the 2% level can be envisaged, with calibration to at least 5% over the next decade appearing straightforward.

Systematic uncertainties are present in both the normalization and evolution of the gas depletion parameter. Writing $\Upsilon(z) = \Upsilon_0(1 + \alpha_\Upsilon z)$, the hydrodynamic simulations of Planelles et al. (2013) and Battaglia et al. (2012) show that for the most massive clusters and for measurement shells $0.8\text{--}1.2 r_{2500}$, $\Upsilon_0 = 0.845 \pm 0.042$ and $\alpha_\Upsilon = 0.00 \pm 0.05$ (uniform priors; Mantz et al. 2013). These priors span the full range of current systematic uncertainty. Our pessimistic assumption for future analyses employs these same conservative priors, whereas our optimistic scenario assumes a 2.5 times reduction in their ranges. We note that our prior on α_Υ also serves as a catch-all for other small-scale evolutionary biases that may affect the measured f_{gas} value.

Note that the priors on K and $\Upsilon(z)$ only model systematics affecting the mean value of $f_{\text{gas}}(z)$; systematics acting stochastically on a cluster-to-cluster basis will be manifested as intrinsic scatter in the measurements. Our projections for future Chandra data assume an intrinsic scatter in f_{gas} of 7.5% for the $0.8\text{--}1.2 r_{2500}$ measurement shell based on current data ($7.4\% \pm 2.3\%$; Mantz et al. 2013), corresponding to an intrinsic scatter in distance of $\sim 5\%$, in both the pessimistic and optimistic scenarios.

5.3.2 XSZ method

The calibration prior for the XSZ analysis, $k(z)$, is set by the accuracy of the temperature and flux calibration for the X-ray and mm instruments. On the X-ray side, the temperature calibration is likely to see near-term improvements through the availability of independent temperature measurements based on X-ray emission line ratios, provided by the ASTRO-H satellite (Takahashi et al. 2010; these will augment the standard temperature estimates based on the shape of the bremsstrahlung continuum). Gravitational lensing data will also play a role. Our pessimistic assumption for this calibration prior assumes a combined systematic uncertainty in future XSZ measurements of 5%, shrinking to 2% in the optimistic case. For the relevant radial range of relaxed clusters, we do not expect these systematics to be redshift-dependent, to first order. To be conservative, however, we also adopt 5% and 2% uncertainties on α_k in the pessimistic and optimistic cases, respectively. In all cases, we assume an intrinsic scatter in the XSZ measurements of 20% (corresponding to 40% in distance; Bonamente et al. 2006; Hallman et al. 2007; Shaw, Holder & Bode 2008). We note, however, that this scatter has yet to be investigated in detail for hot, relaxed clusters specifically, and it is possible that our assumption may overestimate the true level of intrinsic scatter.

5.4 Simulation results

Fig. 4 shows the predicted constraints from the simulated Chandra f_{gas} data set (93 clusters; 53 new, 40 existing) for the non-flat Λ CDM, flat w CDM and flat evolving- w models. Future-optimistic priors are assumed. The results from current f_{gas} data are also shown for comparison. (Note that only cluster f_{gas} data, in conjunction with priors on $\Omega_b h^2$ and h , are used here.) Figures of merit for each model in the future-pessimistic and future-optimistic cases, normalized to the present results, are shown in Table 3. Note also the tight constraint on Ω_m achievable with the f_{gas} experiment (at the $\sim 5\%$ level, optimistically), which is largely independent of the cosmological model assumed. Intuitively, this constraint originates from the fair sample argument and the normalization of the $f_{\text{gas}}(z)$ curve, as described by equation 4.

To date, XSZ data have only been able to constrain h with all other cosmological parameters fixed (e.g. Bonamente et al. 2006). For this highly restricted model the constraints on h from

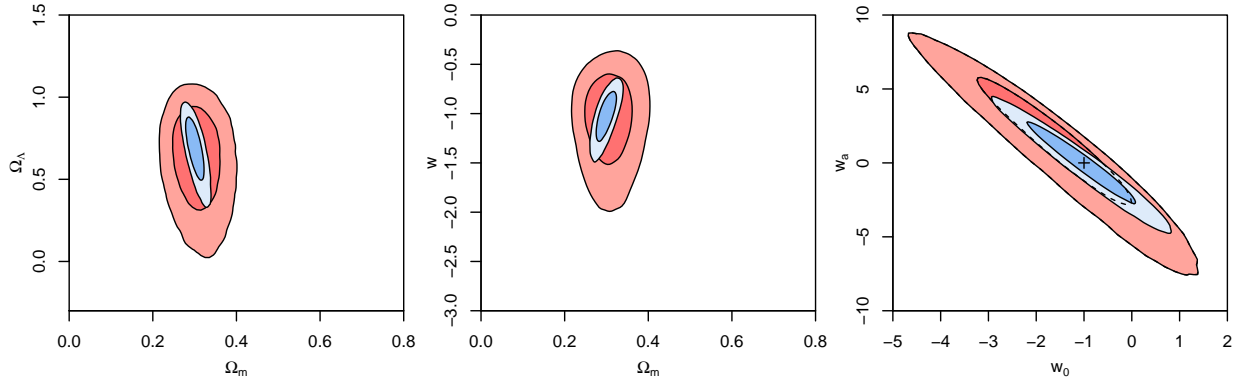


Figure 4: Joint 68.3% and 95.4% confidence constraints from the f_{gas} test for non-flat Λ CDM (left), flat w CDM (center) and flat evolving- w (right) models. Red shading shows the constraints from current f_{gas} data (Mantz et al. 2013; also employing standard priors on $\Omega_b h^2$ and h , as described in the text). Blue shading shows the predicted, improved constraints when adding Chandra data for 53 more clusters, assuming the redshift distribution shown in Fig. 3(b) and f_{gas} measurements to $\sim 15\%$ precision. Optimistic priors are assumed (see Table 1). The cross in the right panel marks the cosmological constant model ($w_0 = -1$, $w_a = 0$).

Table 3: Figures of merit for the f_{gas} experiment, from the combination of current data and 53 additional clusters observed with Chandra. Our figure of merit is defined as the inverse of the area enclosed by the 95.4% confidence contour for the associated pair of parameters, normalized by the constraints provided by current data. The last column lists the fractional constraint on Ω_m .

Model	Parameters	Priors	FoM _c	$\Delta\Omega_m/\Omega_m$
non-flat Λ CDM	$\Omega_m - \Omega_\Lambda$	pessimistic	2.2	0.08
		optimistic	5.8	0.05
flat w CDM	$\Omega_{\text{DE}} - w$	pessimistic	2.3	0.08
		optimistic	6.2	0.05
flat evolving- w	$w_0 - w_a$	pessimistic	2.3	0.12
		optimistic	3.5	0.09

our simulated XSZ data set, which involves 500 clusters measured to 20% precision, approach the systematic limit imposed by $k(z)$, i.e. $\Delta h \geq 2\Delta k_0$ (considering k_0 alone). Interestingly, the simulated XSZ data are also able to constrain Ω_m , albeit weakly. The left panel of Fig. 5 shows the joint constraints on h and Ω_m for a flat Λ CDM model. Table 4 summarizes the constraints on h for this and other models, including non-flat Λ CDM and flat w CDM. (These constraints would be stronger if the intrinsic scatter in XSZ measurements turns out to be smaller than we have assumed.)

5.5 f_{gas} measurements with a next generation X-ray observatory

The program of observations described above, which involves $\sim 5\%$ of the available Chandra observing time over the next decade (~ 10 Ms), is ambitious but achievable given sufficient community support. However, expanding the scope of this work yet further will be difficult, with observing time on flagship X-ray observatories likely to be the limiting factor. Longer term, the full exploitation of the f_{gas} technique, which might involve e.g. doubling the precision of the individual measurements (to approach the systematic limit) and quadrupling the sample size considered here, will require a new flagship X-ray observatory with greater collecting area than Chandra. Possibilities include the

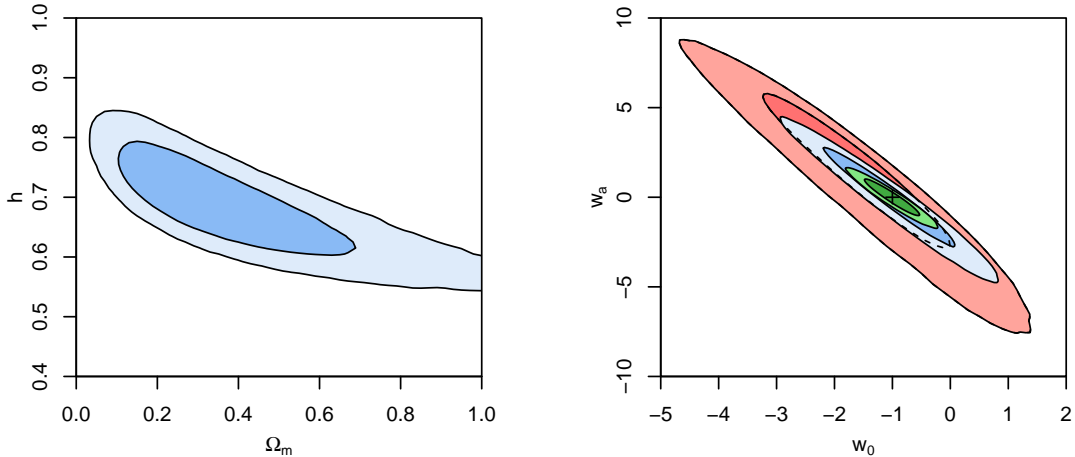


Figure 5: (*a; left panel*) Predicted 68.3% and 95.4% confidence constraints on the Hubble parameter and mean matter density from a future XSZ experiment, utilizing relatively short X-ray observations and follow-up mm-wavelength data for 500 clusters. A flat Λ CDM model and optimistic priors (see text) are assumed. (*b; right panel*) Predicted 68.3% and 95.4% confidence constraints for a more ambitious, future f_{gas} experiment using a next-generation X-ray observatory with 30 times the collecting area of Chandra (green inner curves; the outer red and blue curves are reproduced from Fig. 4). The experiment involves deep X-ray observations for 450 clusters, providing f_{gas} measurements to 7.5% precision, and assumes 5% intrinsic scatter. A flat, evolving- w model and optimistic priors (see text) are assumed.

Table 4: Fractional, marginalized constraints on h ($\Delta h/h$) provided by the simulated XSZ data.

Model	$\Delta h/h$	
	pessimistic	optimistic
only h free	0.11	0.05
flat Λ CDM	0.12	0.09
non-flat Λ CDM	0.13	0.09
flat w CDM	0.18	0.16

SMART-X mission (<http://hea-www.cfa.harvard.edu/SMARTX/>) and ATHENA+ (Nandra et al., 2013).

To explore the potential of such an observatory for f_{gas} work, we have simulated a data set that could be gathered by an observatory with comparable spatial resolution to Chandra but ~ 30 times the collecting area (other instrument characteristics are assumed to be the same, in the pessimistic case). The target clusters are again drawn fairly from the distribution shown in Fig. 3a, with the requirement that $z \geq 0.3$. In this case, however, the simulated f_{gas} measurements have a precision of 7.5%, approximately matching the observed level of the intrinsic scatter in current data. Adopting a 10 Ms observing budget, more than 400 new clusters could be observed, providing a total sample of ~ 450 clusters with f_{gas} measured to this precision.

Our pessimistic projections for this future observatory assume an intrinsic scatter in f_{gas} of 7.5%. In the optimistic case, we assume that measurements of bulk and turbulent gas velocities with high resolution X-ray spectrometers will allow us to reduce this scatter to 5%. (Bulk and turbulent motions are expected to contribute significantly to the observed intrinsic scatter in f_{gas} ; e.g. Nagai, Vikhlinin & Kravtsov 2007; Battaglia et al. 2012.)

The cosmological constraints for a flat, evolving- w model in the optimistic case are shown in the right panel of Fig. 5. (Again, only cluster f_{gas} data and priors on $\Omega_b h^2$ and h are used.) Figures of merit, normalized to the present results, are shown in Table 5, and are a further factor of 6–7

Table 5: As for Table 3, but for f_{gas} measurements made with a future X-ray observatory. The simulated data set includes 450 clusters with f_{gas} measured to 7.5% precision, and assumes an intrinsic scatter of 5.0%.

Model	Parameters	Priors	FoM _c	$\Delta\Omega_{\text{m}}/\Omega_{\text{m}}$
flat evolving- w	$w_0 - w_a$	pessimistic	16.7	0.10
		optimistic	22.6	0.06

tighter than those for the 10 Ms Chandra program described above.

Given the substantial expected intrinsic scatter in XSZ measurements, the impact of a new X-ray observatory on that test is likely to be relatively modest and we do not consider it further here.

6 Conclusions

We have examined the ability of current and near-term multiwavelength observations of galaxy clusters to measure cosmic distances and constrain cosmology via the f_{gas} and XSZ experiments. Existing f_{gas} measurements for hot ($kT > 5$ keV), dynamically relaxed clusters (~ 40 systems, mostly at $z \leq 0.6$; Mantz et al. 2013 and references therein) provide competitive constraints on dark energy, comparable to those from current BAO and SNIa studies. Expanding this work to include measurements for approximately 100 such clusters, spanning the redshift range $0 < z < 1.4$, with f_{gas} measured to a precision of 15% in the $0.8\text{--}1.2 r_{2500}$ shell, should constrain dark energy with a figure of merit 4 – 6 times better, depending on the cosmological model. In particular, the f_{gas} data provide a tight constraint on Ω_{m} , independent of the cosmological model assumed. Our projections assume modest improvements in hydrodynamical simulations and weak lensing mass calibration, and the availability of approximately 5% of the total Chandra observing budget (~ 10 Ms) for this work over the next decade, noting that these Chandra observations will also facilitate a broad range of astrophysical studies. We assume a redshift distribution of the observed clusters that is representative of the population that eROSITA will find, although in practice this redshift distribution could be further optimized for dark energy studies.

In determining our predicted dark energy constraints we have employed the same MCMC method used to analyze current data. This encapsulates all of the relevant degeneracies between parameters and allows one to easily and efficiently incorporate priors and systematic allowances in the analysis.

The availability of observing time on major X-ray observatories such as Chandra and XMM-Newton is likely to be the limiting factor for the $f_{\text{gas}}(z)$ experiment. Longer term, the full exploitation of this technique will require a new flagship X-ray observatory with comparable spatial resolution but greater collecting area than Chandra. We have considered the prospects for distance measurements with such an observatory, demonstrating that the constraints on evolving dark energy models are likely to be improved by a further factor of 6 – 7.

We conclude that the f_{gas} and XSZ experiments offer a powerful approach for measuring cosmic distances which should be competitive with and complementary to other leading methods over the next decade.

Acknowledgments

This work was supported in part by the US Department of Energy under contract number DE-AC02-76SF00515, by the National Aeronautics and Space Administration through Chandra Award

Numbers GO8-9118X and TM1-12010X, and by the National Science Foundation under grants AST-0838187 and AST-1140019. The Dark Cosmology Centre (DARK) is funded by the Danish National Research Foundation.

References

- Albrecht A, Bernstein G, Cahn R, Freedman WL, Hewitt J, et al. 2006. *arXiv:astro-ph/0609591*
- Allen SW, Evrard AE, Mantz AB. 2011. *ARA&A* 49:409–470
- Allen SW, Rapetti DA, Schmidt RW, Ebeling H, Morris RG, Fabian AC. 2008. *MNRAS* 383:879–896
- Allen SW, Schmidt RW, Ebeling H, Fabian AC, van Speybroeck L. 2004. *MNRAS* 353:457–467
- Anderson L, Aubourg E, Bailey S, Beutler F, Bolton AS, et al. 2013. *arXiv:1303.4666*
- Applegate DE, von der Linden A, Kelly PL, Allen MT, Allen SW, et al. 2012. *arXiv:1208.0605*
- Applegate et al. 2013. in preparation
- Battaglia N, Bond JR, Pfrommer C, Sievers JL. 2012. *arXiv:1209.4082*
- Benson BA, de Haan T, Dudley JP, Reichardt CL, Aird KA, et al. 2013. *ApJ* 763:147
- Bonamente M, Joy MK, LaRoque SJ, Carlstrom JE, Reese ED, Dawson KS. 2006. *ApJ* 647:25–54
- Carlstrom JE, Holder GP, Reese ED. 2002. *ARA&A* 40:643–680
- Dunkley J, Komatsu E, Nolta MR, Spergel DN, Larson D, et al. 2009. *ApJS* 180:306–329
- Ettori S, Morandi A, Tozzi P, Balestra I, Borgani S, et al. 2009. *A&A* 501:61–73
- Freedman WL, Madore BF, Gibson BK, Ferrarese L, Kelson DD, et al. 2001. *ApJ* 553:47–72
- Giodini S, Pierini D, Finoguenov A, Pratt GW, Boehringer H, et al. 2009. *ApJ* 703:982–993
- Hallman EJ, O’Shea BW, Burns JO, Norman ML, Harkness R, Wagner R. 2007. *ApJ* 671:27–39
- Hinshaw G, Larson D, Komatsu E, Spergel DN, Bennett CL, et al. 2012. *arXiv:1212.5226*
- Kelly PL, von der Linden A, Applegate DE, Allen MT, Allen SW, et al. 2012. *ArXiv e-prints*
- Kowalski M, Rubin D, Aldering G, Agostinho RJ, Amadon A, et al. 2008. *ApJ* 686:749–778
- LaRoque SJ, Bonamente M, Carlstrom JE, Joy MK, Nagai D, et al. 2006. *ApJ* 652:917–936
- Lewis A, Bridle S. 2002. *Phys. Rev. D* 66:103511
- Mantz A, Allen SW, Ebeling H, Rapetti D, Drlica-Wagner A. 2010a. *MNRAS* 406:1773–1795
- Mantz A, Allen SW, Rapetti D. 2010. *MNRAS* 406:1805–1814
- Mantz A, Allen SW, Rapetti D, Ebeling H. 2010b. *MNRAS* 406:1759–1772
- Mantz et al. 2013. in preparation

McDonald M, Benson BA, Vikhlinin A, Stalder B, Bleem LE, et al. 2013. *ArXiv e-prints*

Merloni A, Predehl P, Becker W, Böhringer H, Boller T, et al. 2012. *arXiv:1209.3114*

Nagai D, Vikhlinin A, Kravtsov AV. 2007. *ApJ* 655:98–108

Nandra K, Barret D, Barcons X, Fabian A, den Herder JW, et al. 2013. *arXiv:1306.2307*

Percival WJ, Reid BA, Eisenstein DJ, Bahcall NA, Budavari T, et al. 2010. *MNRAS* 401:2148–2168

Pettini M, Cooke R. 2012. *MNRAS* 425:2477–2486

Planelles S, Borgani S, Dolag K, Ettori S, Fabjan D, et al. 2013. *MNRAS* 431:1487–1502

Rapetti D, Allen SW, Mantz A. 2008. *MNRAS* 388:1265–1278

Rapetti D, Allen SW, Mantz A, Ebeling H. 2010. *MNRAS* 406:1796–1804

Rapetti D, Blake C, Allen SW, Mantz A, Parkinson D, Beutler F. 2013. *MNRAS* 432:973–985

Reid BA, Verde L, Jimenez R, Mena O. 2010. *J. Cosmology Astropart. Phys.* 1:3

Riess AG, Macri L, Casertano S, Lampeitl H, Ferguson HC, et al. 2011. *ApJ* 730:119

Rozo E, Wechsler RH, Rykoff ES, Annis JT, Becker MR, et al. 2010. *ApJ* 708:645–660

Santos JS, Tozzi P, Rosati P, Nonino M, Giovannini G. 2012. *A&A* 539:A105

Schmidt F, Vikhlinin A, Hu W. 2009. *Phys. Rev. D* 80:083505

Shaw LD, Holder GP, Bode P. 2008. *ApJ* 686:206–218

Siemiginowska A, Burke DJ, Aldcroft TL, Worrall DM, Allen S, et al. 2010. *ApJ* 722:102–111

Silk J, White SDM. 1978. *ApJL* 226:L103–L106

Sunyaev RA, Zeldovich YB. 1972. *Comments on Astrophysics and Space Physics* 4:173–178

Suzuki N, Rubin D, Lidman C, Aldering G, Amanullah R, et al. 2012. *ApJ* 746:85

Takahashi T, Mitsuda K, Kelley R, Aharonian F, Akimoto F, et al. 2010. In *Society of Photo-Optical Instrumentation Engineers (SPIE) Conference Series*, vol. 7732 of *Society of Photo-Optical Instrumentation Engineers (SPIE) Conference Series*

Tinker J, Kravtsov AV, Klypin A, Abazajian K, Warren M, et al. 2008. *ApJ* 688:709–728

Vikhlinin A, Kravtsov AV, Burenin RA, Ebeling H, Forman WR, et al. 2009. *ApJ* 692:1060–1074

von der Linden A, Allen MT, Applegate DE, Kelly PL, Allen SW, et al. 2012. *ArXiv e-prints*

Weinberg DH, Mortonson MJ, Eisenstein DJ, Hirata C, Riess AG, Rozo E. 2012. *arXiv:1201.2434*

White SDM, Navarro JF, Evrard AE, Frenk CS. 1993. *Nat* 366:429–433

Wolz L, Kilbinger M, Weller J, Giannantonio T. 2012. *J. Cosmology Astropart. Phys.* 9:9

Wu H, Rozo E, Wechsler RH. 2010. *ApJ* 713:1207–1218